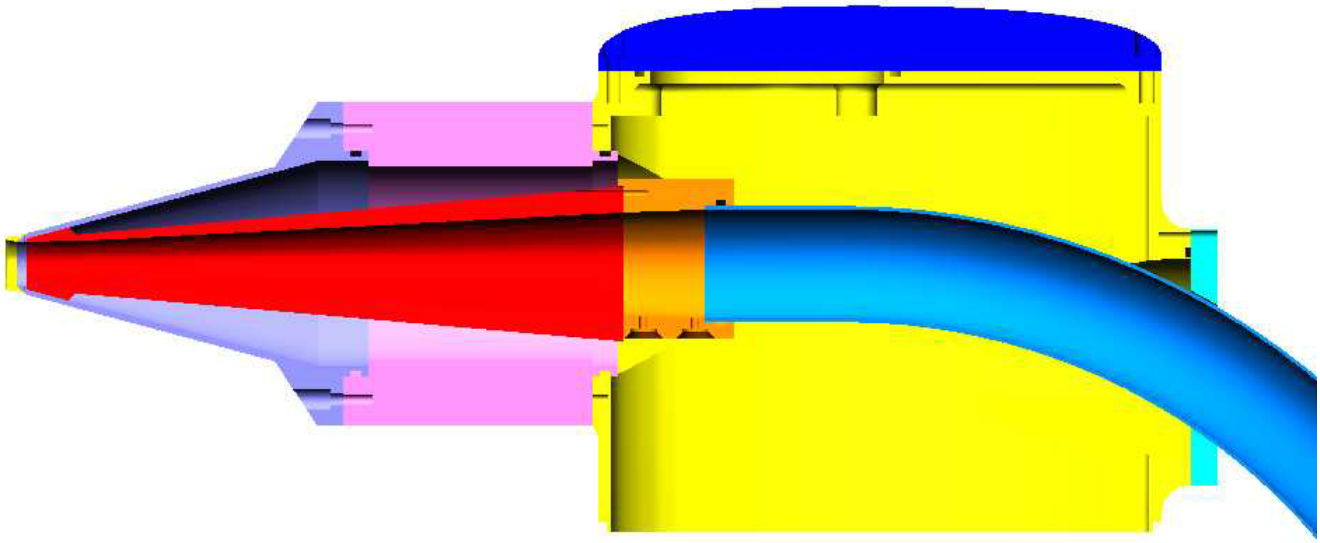

Figure S1. Detail of the LTI. Porous diffuser is red, with suction plenums above and below connected to the yellow strut plenum. Sample flow passes through the curved blue tubing to enter the fuselage (below the bottom of the figure). When in use, the hot film anemometer probe is located in the left center of the orange section. The yellow section on the inlet tip is the elliptically-curved blunt leading edge.

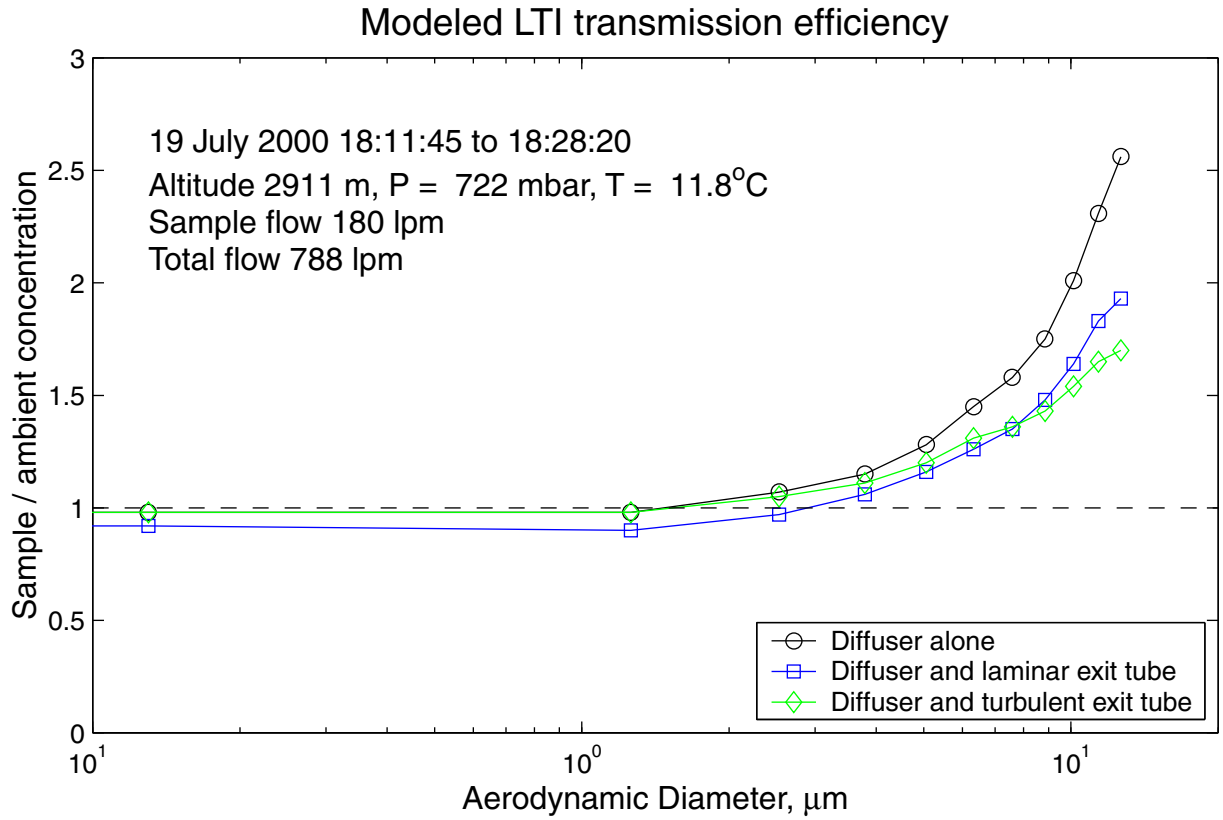

Figure S2. Fluent modeling of the enhancement in LTI sample flow due to inertial separation of particles from curving streamlines. Black circles: enhancement only. Blue squares: enhancement and losses in exit bend assuming laminar flow. Green diamonds: enhancement and losses assuming turbulent flow in exit bend. Modeling by D. Gesler.

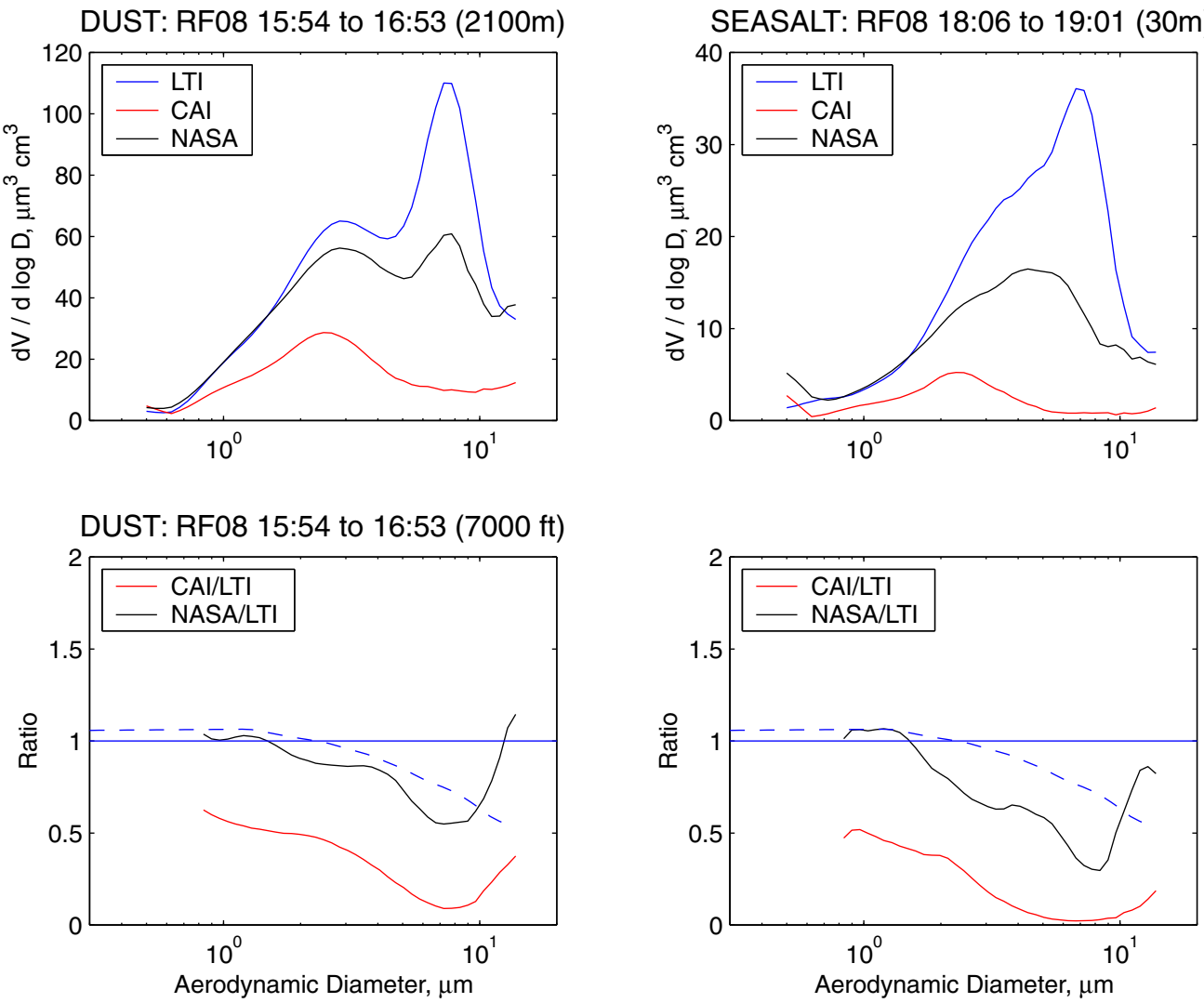

Figure S3. Typical APS data behind the three inlets. The left panels are for a flight leg in dust, while the right panels are for a MBL leg. In the top panels are volume distributions for the three inlets. As in every leg, the LTI admitted the most particles, then the SD and finally the CAI. We frequently observed two modes in the volume distribution, one peaking around 2-4 um and the other peaking at 6-8 um. The SD efficiency was closer to that of the LTI in dry dust legs than in the humid MBL. The lower panels show the ratios of the concentration at each size behind the other inlets to concentrations behind the LTI. The dotted lines are the reciprocal of the enhancement and loss (Fig. S2), to clarify how much of the observed differences might be due to enhancement by the LTI.

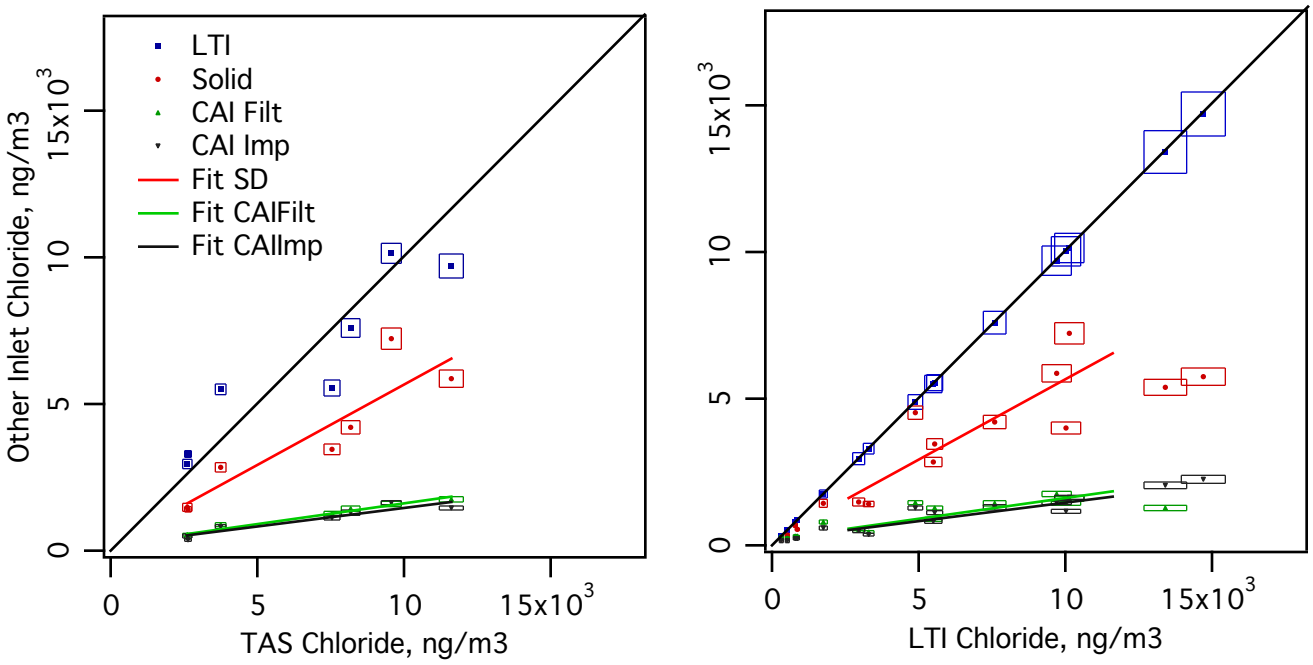

Figure S4. A comparison of choride on filters behind the various inlets vs TAS Cl- (left panel) and LTI Cl (right). Linear fits are shown for the SD, CAI impactor, and CAI filter data. Boxes represent uncertainties derived from twice the blank variability, the detection limit, and flow uncertainty. The LTI reproduces the ambient chloride (represented by TAS) within 10-20%, while the other inlets are bised lower.

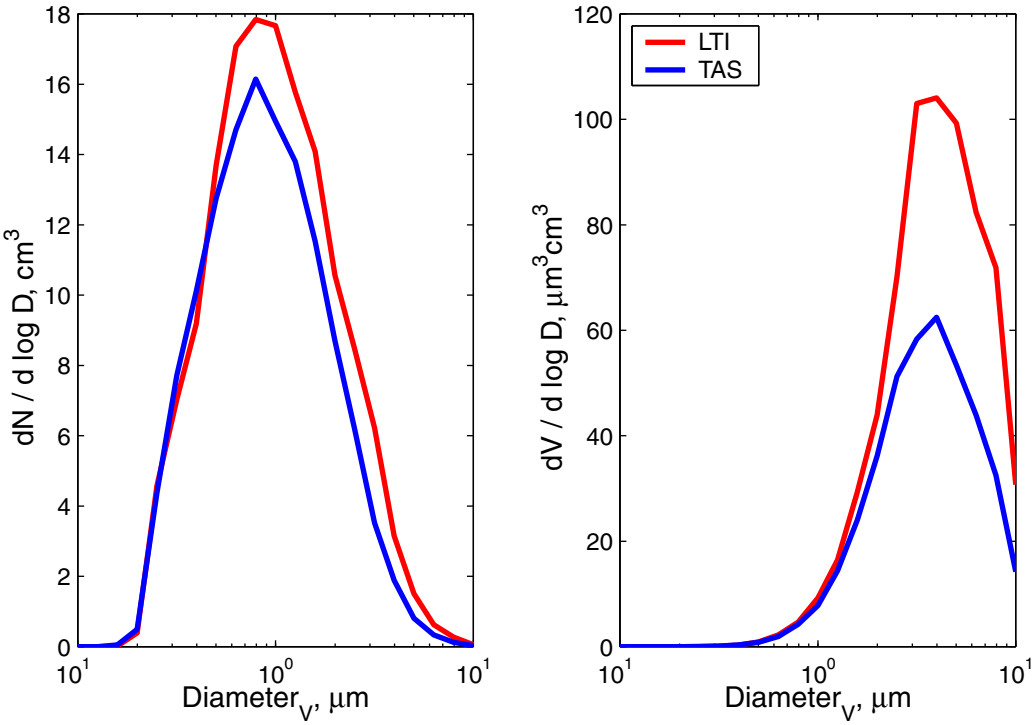

Figure S5. Comparison of SEM-derived size distributions behind the LTI and in TAS. The left panel is a number distribution, while the right is a volume distribution. The diameter was derived from an estimate of the volume of each particle. No corection has been made for the enhancement by the porous diffuser.

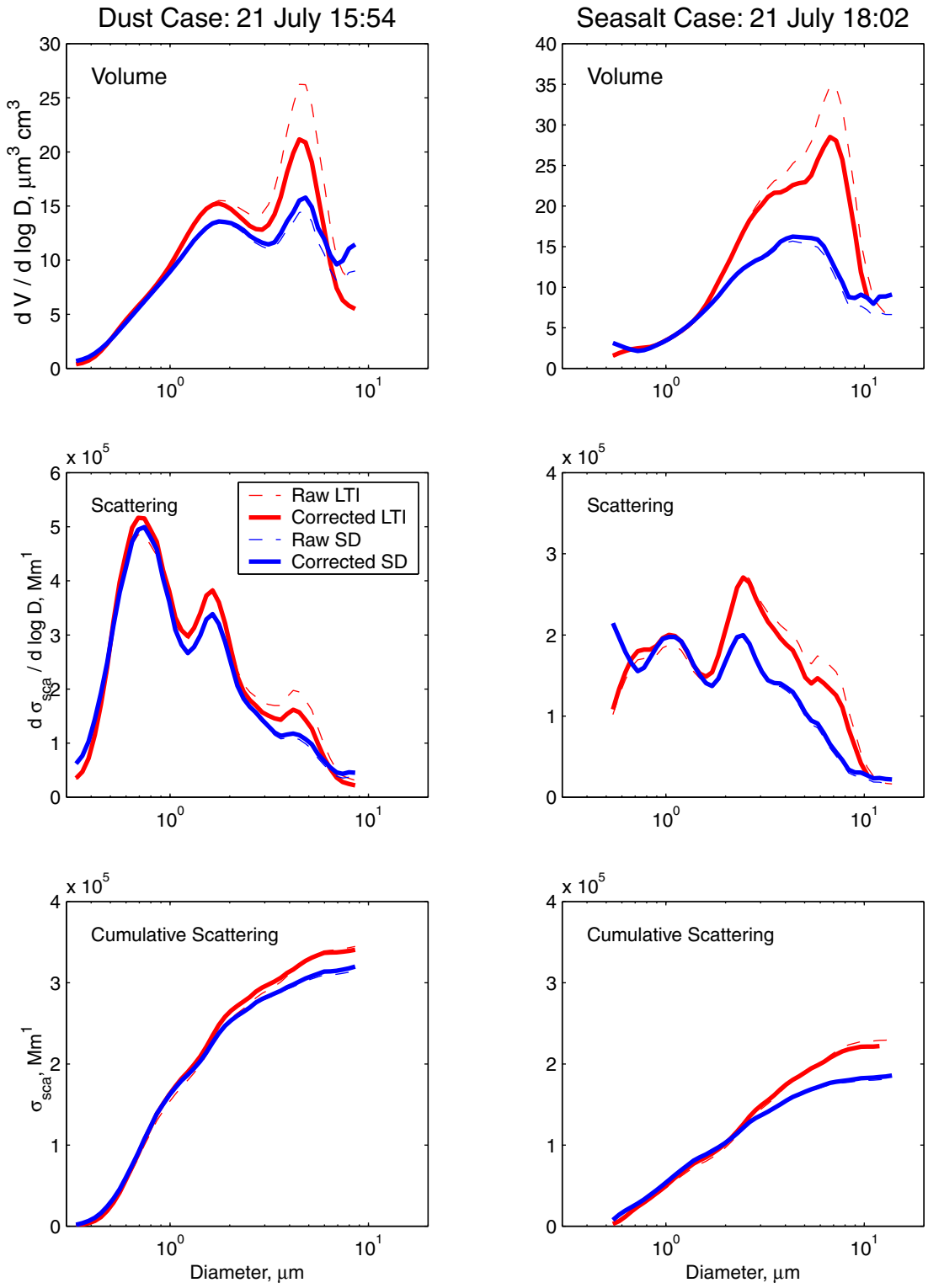

Figure S6. Accuracy of derived optical properties from the LTI and SD. The left panels are for a dry dust case, the right panels for a sea salt leg. The top panels show the best-guess corrections of both inlets for enhancement and tubing losses. The second panels use Mie theory to compute the scattering based on the size distributions and assumtions about the density and refractive indices of dust and sea salt. The bottom panels show the cumulative scattering. The leveling off at larger sizes is due to the fact that the mass scattering efficiency drops for larger particles, so they have little radiative impact.